Laser-induced fluorescence of NCN in low and atmospheric pressure flames

R. J. H. Klein-Douwel,* N. J. Dam, and J. J. ter Meulen

Applied Molecular Physics, Institute for Molecules and Materials, Radboud University Nijmegen, P.O. Box 9010, 6500 GL Nijmegen, The Netherlands

**Corresponding author: R.Klein-Douwel@science.ru.nl*

Received July 31, 2008; revised September 17, 2008; accepted September 23, 2008; posted October 8, 2008 (Doc. ID 99611); published November 11, 2008

The cyanonitrene radical, NCN, is detected by laser-induced fluorescence in laminar, adiabatic, flat $\phi=1.3$ methane–air flames at 200 hPa and atmospheric pressure. Laser excitation of the $\tilde{A}^3\Pi_u(020)$–$\tilde{X}^3\Sigma_g^-(000)$ band at 317 nm allows off-resonant fluorescence to be detected at 326 nm. Excitation and dispersed fluorescence spectra are presented, as well as profiles of NCN and CH versus height above burner.

OCIS codes: 120.1740, 300.6170, 300.2530, 300.6540, 280.2470, 280.1740.

Prompt NO formation in combustion processes has been relatively well-understood since the early work of Fenimore [1]. The rate-limiting reaction has long been thought to be $CH+N_2 \leftrightarrow HCN+N$. Recently, however, it has been found that this reaction, which is spin forbidden, has to be replaced by $CH+N_2 \leftrightarrow NCN+H$ [2]. By now, this reaction is being incorporated in chemical mechanisms [3–5]. The importance of NCN in combustion processes has also been derived from studies on NO [6] and HCN [7].

The spectroscopy of NCN has been pioneered by Herzberg and Travis [8] and later expanded by, e.g., Kroto *et al.* [9], Smith and co-workers [10], and Beaton *et al.* [11]. Its diagonal transitions [e.g., (000)–(000) or (020)–(020)] are much stronger than the off-diagonal ones [e.g., (020)–(000)]. NCN has been observed in emission of flames containing active nitrogen [12] or cyanogen [13] and in comets [14].

NCN has first been observed in flames by laser-induced fluorescence (LIF) by Smith [15], using a methane–air flame with fuel equivalence ratio $\phi=1.3$ at 40 hPa. In that study, NCN is excited in the 327–329 nm range, where the signals are due to the $\tilde{A}^3\Pi_u(000)$–$\tilde{X}^3\Sigma_g^-(000)$ band and (010)–(010) hot bands. The LIF wavelength of these bands is (almost) resonant with the excitation wavelength. More recently, NCN LIF has been detected in very similar flames [16,17] (at 40 and 53 hPa, respectively) and in a shock tube [18], using the same transitions. In [16,18] the signal is assigned to NCN based on the excitation wavelength of 329.13 nm. Nearby OH LIF is employed in [16] to obtain semiquantitative NCN mole fractions, while use of cavity ringdown spectroscopy and spectral simulation yielded an absolute NCN concentration of 170 ± 90 parts in 10^9 (ppb) in the flame used in [17].

Elastic light scattering is manageable at the low pressures used in [15–17], but at higher pressures, more realistic for practical combustion applications, it becomes problematic. This can be avoided by using the NCN $\tilde{A}^3\Pi_u(020)$–$\tilde{X}^3\Sigma_g^-(000)$ band, as suggested in [10] (but not observed in [15]). The current Letter describes the first LIF detection of this band in flames (at 200 hPa and atmospheric pressure), and excitation and dispersed fluorescence spectra are compared to data in [10]. Since insufficient spectroscopic data is known for this band (in contrast to the bands used in [15–18]), results presented here must remain qualitative.

The burner system is almost identical to the one described in [19]; some details are given here. The burner deck consists of a perforated plate of 30 mm diameter (0.5 mm diameter holes at 0.7 mm pitch) and the flows of methane and air are computer-controlled by mass flow controllers. The burner deck is preheated by an outer ring to compensate for heat loss of the flame to the burner deck, and thermocouples are used for checking adiabaticity. The entire burner system is mounted on a calibrated vertical translator. The height-above-burner h_{ab} of the laser beam (derived from Rayleigh scattering) is measured with a camera system (described below). Measurements have been performed in laminar, $\phi=1.3$, methane–air flames at pressures of 200 and 1000 hPa. At the latter (atmospheric) pressure, the flame front is thinner and closer to the burner. Results are shown for a pressure of 200 hPa, unless stated otherwise.

The $\tilde{A}^3\Pi_u(020)$–$\tilde{X}^3\Sigma_g^-(000)$ band of NCN is excited at 316.970 nm [10] by frequency doubling (in a KDP crystal) the output of a Nd:YAG-pumped tunable dye laser [Quantel YG781C10 (5 ns pulse) and Quantel TDL50, respectively] operating on a mixture of 4-dicyanomethylene-2-methyl-6-(*p*-dimethylaminostyryl)-4*H*-pyran (DCM) and pyridine-1 dyes dissolved in ethanol. The resulting ultraviolet laser light is focused above the burner by an $f=430$ mm lens and has a FWHM diameter of 0.7 mm. The laser beam polarization is such that detection of Rayleigh scattering is minimized, but it is still significant. The laser power is 50–100 μJ/pulse, so saturation is not expected to happen for NCN or CH, but may occur for OH (which is recorded for wavelength calibration purposes only). Since the selected NCN band is relatively weak, higher laser powers may be used while still avoiding saturation.

The LIF signal is observed at right angles to the laser beam with an intensified CCD camera (Princeton Instruments THM, 512×512 pixels, 16-bit dynamic range), which is mounted behind a spectrograph (Acton SP300i) equipped with a UV Nikkor $f=105$ mm, $f/4.5$ lens. The spectrograph entrance slit is parallel to the laser beam and the burner deck. Dispersed fluorescence spectra have been taken with a 2400 grooves/mm grating, yielding a total view of about 18.8 nm in one direction of the camera image (0.037 nm/pixel). The perpendicular image direction represents spatial information (at 0.15 mm/pixel) and captures more than the entire width of the flame. To increase the signal–noise ratio, however, spectra have been recorded while binning together pixels in the spatial direction over almost the entire width of the flame. In this way dispersed fluorescence spectra could be recorded rapidly and continuously while the laser excitation wavelength was scanned slowly, yielding two-dimensional excitation–dispersion spectra. Figure 1 presents an example of this, in which 100 laser shots are integrated per dispersed fluorescence spectrum. From these spectra separate excitation and dispersed fluorescence spectra are easily obtained. The spectrograph–camera combination is also used to record the position of the flame front, using CH^* chemiluminescence as a marker.

The LIF signal of NCN and spectrally nearby transitions of OH (A–X system) and CH (C–X system) are recognizable in Fig. 1 and the wavelengths of OH and CH lines are used for accurate spectral calibration of both wavelength axes using LIFBASE [20]. Employing an excitation–dispersion spectrum, as displayed in Fig. 1, shows that in case of nearly equal excitation wavelengths, species can still be identified and spectrally separated by their dispersed fluorescence wavelengths. Reference measurements of CH LIF are performed by exciting the $P_1(9)(0,0)$ C–X transition at 316.943 nm. The population of the lower level of this transition is relatively insensitive to temperature variations in the range encountered in this flame, so that its intensity is a coarse measure of the local CH density.

An excitation spectrum of the $\tilde{A}$–$\tilde{X}$ (020)–(000) band head of NCN at 316.970 nm [10], derived from Fig. 1, is presented in Fig. 2. Only fluorescence between 325.67 and 326.00 nm is selected for extracting the excitation spectrum. The $P_2(15)$ (0,0) and

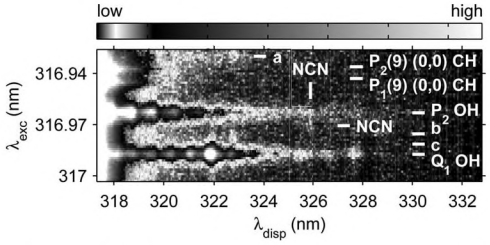

Fig. 1. Excitation–dispersion spectrum, recorded at the flame front. LIF features originating from NCN, CH, and OH are identified: NCN and P_2/Q_1 OH are explained in Fig. 2; $a=P_{12}(15)$ (0,0) OH, $b/c=Q_1/Q_2(21)$ (1,1) CH (λ_{disp} =322.7 nm for a–c). Low intensities are enhanced in a nonlinear way (detector saturated near laser wavelength).

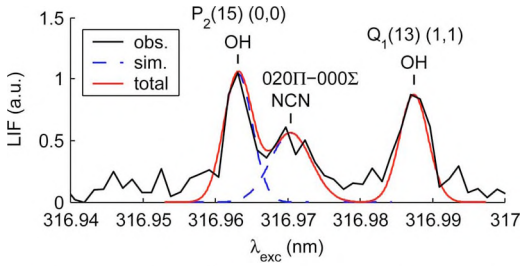

Fig. 2. (Color online) Excitation spectrum of the NCN $\tilde{A}^3\Pi_u(020)$–$\tilde{X}^3\Sigma_g^-(000)$ band head.

$Q_1(13)$ (1,1) transitions of OH are detected as well. The spectral lines are simulated by Gaussian curves. For OH a FWHM of 0.0047 nm is used (consistent with nearby OH lines not shown here), for NCN a FWHM of 0.0067 nm is used. It must be noted that at $\lambda_{exc}=316.966$ nm both the $O_{12}(4)$ (1,1) transition of OH and the $O_{12}(5)$ (0,0) transition of CH can be excited, but the fluorescence of both these two lines is blueshifted relative to the excitation wavelength and therefore not present in the excitation spectrum in Fig. 2.

Dispersed fluorescence spectra are recorded at the flame front by integrating 1800 laser shots at a fixed $\lambda_{exc}=316.970$ nm. Figure 3 shows the results in the 200 hPa and atmospheric pressure flames. Two separately recorded spectra are shown for each pressure, indicating good reproducibility. The NCN fluorescence at 325.90 nm most likely originates from the (020)–(020) band [10] and is clearly visible in the 200 hPa spectrum and still present (but harder to see) in the 1000 hPa spectrum. Both the excitation and maximum fluorescence wavelengths correspond very well to literature values [10], thereby confirming the assignment of these signals as belonging to NCN. Other NCN transitions in the region $315 \leqslant \lambda_{exc} \leqslant 320$ nm (the weaker features in [10]) could not be detected in the flame.

Use of the current detection scheme, which has a maximum fluorescence signal at a wavelength clearly separated from the excitation wavelength, allows detection of NCN under (flame) conditions where elastic laser light scattering may be too large for resonant detection, that is at higher pressures or very close to a surface. These last two conditions both apply to the measurements at atmospheric pressure presented here, but in this case LIF of NCN can still be detected at the flame front because a spectrograph is used.

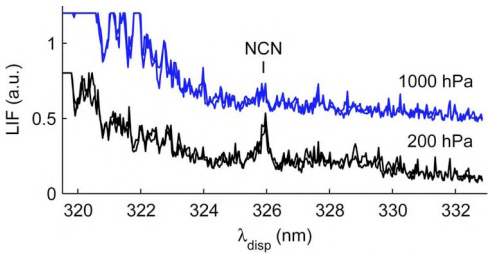

Fig. 3. (Color online) Spectra of dispersed fluorescence following excitation of the $\tilde{A}$–$\tilde{X}$ (020)–(000) head (two spectra at each pressure, vertical offset between pressures for clarity; detector saturated for $\lambda_{disp} \leqslant 320$ nm).

The thickness of the flame front and its separation from the burner allow dispersed fluorescence spectra of NCN to be recorded versus h_{ab} at 200 hPa. To this end, a linear background is fit and the remaining net signal between 325.71 and 326.07 nm is integrated. A similar procedure is followed for dispersed fluorescence spectra of CH after exciting the $P_1(9)(0,0)$ C–X transition. In this case the net signal of the Q branch is integrated between 313.87 and 314.79 nm, with integration of 200 laser shots per spectrum being sufficient. The resulting variations of net NCN and CH signals with h_{ab} are shown in Fig. 4.

From this data it is clear that the NCN signal peaks somewhat higher above the burner than CH, that the NCN distribution is somewhat narrower than that of CH, and also that the presence of NCN is limited to the flame front. These results are similar to those observed in [15–17]. In those studies the FWHM of the NCN distribution is slightly larger than 2 mm (at $\leqslant$53 hPa), whereas here it is about 0.9 mm at 200 hPa. This difference is caused by the higher pressure. The h_{ab} of maximum NCN signal presented here differs from that in [15–17], but apart from pressure effects this may be due to different burner–flame conditions in those studies.

In summary, clear spectra of the NCN $\tilde{A}^3\Pi_u(020)$–$\tilde{X}^3\Sigma_g^-(000)$ band have been recorded in a ϕ=1.3 methane–air flame at both 200 hPa and atmospheric pressure. This extends NCN measurements to higher pressures than reported in earlier literature [15–17]. Using the off-resonant excitation–detection scheme presented here (λ_{exc}=316.970 nm and λ_{disp}=325.90 nm) allows unambiguous detection of NCN [10]. It also allows NCN LIF to be measured in situations with more laser light scattering, either from Rayleigh scattering at higher pressures or reflections off surfaces. Variation of the NCN signal (with respect to that of CH) with the height above the burner, as observed here at 200 hPa, is similar to that presented in [15–17].

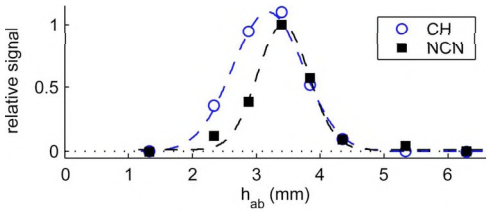

Fig. 4. (Color online) NCN and CH LIF signal versus h_{ab} in the 200 hPa flame. Gaussian fits guide the eye.

Discussions with A. A. Konnov (Vrije Universiteit Brussel and Technische Universiteit Eindhoven) are gratefully acknowledged, as is technical support from L. Gerritsen and A. P. van Vliet and financial support from the Technology Foundation Stichting Technische Wettenschappen.

References

1. C. P. Fenimore, Proc. Combust. Inst. **13**, 373 (1971).
2. L. V. Moskaleva and M. C. Lin, Proc. Combust. Inst. **28**, 2393 (2000).
3. A. El bakali, L. Pillier, P. Desgroux, B. Lefort, L. Gasnot, J. F. Pauwels, and I. da Costa, Fuel **85**, 896 (2006).
4. J. A. Sutton and J. W. Fleming, Combust. Flame **154**, 630 (2008).
5. A. A. Konnov, "Implementation of the NCN pathway of prompt-NO formation in the detailed reaction mechanism" (submitted to Combust. Flame).
6. B. A. Williams and J. W. Fleming, Proc. Combust. Inst. **31**, 1109 (2007).
7. S. Gersen, A. V. Mokhov, and H. B. Levinsky, Combust. Flame **155**, 267 (2008).
8. G. Herzberg and D. N. Travis, Can. J. Phys. **42**, 1658 (1964).
9. H. W. Kroto, T. F. Morgan, and H. H. Sheena, Trans. Faraday Soc. **66**, 2237 (1970).
10. G. P. Smith, R. A. Copeland, and D. R. Crosley, J. Chem. Phys. **91**, 1987 (1989).
11. S. A. Beaton, Y. Ito, and J. M. Brown, J. Mol. Spectrosc. **178**, 99 (1996).
12. K. R. Jennings and J. W. Linnett, Trans. Faraday Soc. **56**, 1737 (1960).
13. E. M. Bulewicz, Proc. Combust. Inst. **12**, 957 (1969).
14. J. H. Valk, C. R. O'Dell, A. L. Cochran, W. D. Cochran, C. B. Opal, and E. S. Barker, Astrophys. J. **388**, 621 (1992).
15. G. P. Smith, Chem. Phys. Lett. **367**, 541 (2003).
16. J. A. Sutton, B. A. Williams, and J. W. Fleming, Combust. Flame **153**, 465 (2008).
17. N. Lamoureux, X. Mercier, C. Western, J. F. Pauwels, and P. Desgroux, Proc. Combust. Inst. **32** (2009), doi:10.1016/j.proci.2008.06.043.
18. V. Vasudevan, R. K. Hanson, C. T. Bowman, D. M. Golden, and D. F. Davidson, J. Phys. Chem. A **111**, 11818 (2007).
19. K. J. Bosschaart and L. P. H. de Goey, Combust. Flame **132**, 170 (2003).
20. J. Luque and D. R. Crosley, *LIFBASE: Database and Spectral Simulation*, Tech. Rep. MP 99-009, SRI International (1999) (version 2.0.60, 2008), http://www.sri.com/psd/lifbase/.